

A novel method to improve the critical damage parameter of powder metallurgical components during the cold upsetting

Proc IMechE Part E:
J Process Mechanical Engineering
0(0) 1–15
© IMechE 2021
Article reuse guidelines:
sagepub.com/journals-permissions
DOI: 10.1177/09544089211020966
journals.sagepub.com/home/pie



R Tharmaraj¹ , M Joseph Davidson¹ and R Raja²

Abstract

In the metal forming process, the understanding of metal flows and the fracture strains are most significant to the failure/damage of the components. Usually, in metalworking, damage occurs because of nucleation, growth and coalescence of the void into a small fracture. These small fractures increased in the circumferential path due to the existence of stresses and the pores which leads to failure at the equatorial position during the upsetting of porous samples. Hence, the fracture of the workpieces strongly depends on the stresses and the pores. Such form of stresses and pores if relieved will give a better damage limit of the material. Therefore, in this research, a novel scheme of localised heating is adopted at the equatorial position of the compressed samples to enhance the critical damage parameter. The powder metallurgy route was used to prepare the required compacts with different relative densities (80%–90%) and 1 aspect ratio by applying suitable powder forming pressures. The upsetting test was performed on the obtained porous samples for various weight percentages of titanium (2%–6%) in the aluminium at the stable strain rate (0.1 s^{-1}) and the damage location was noticed for various components. After the identification of damage position, various temperatures (100°C – 250°C) of localised heating were attempted on the failure site of the specimens after some incremental stages of upsetting tests. The experimental results were analysed using various damage criteria and it was found that the initiation of failure is delayed and increased the critical damage value by selectively heating the samples because of relieving the stresses, reduction in porosity and changes in microstructure.

Keywords

Aluminium, failure parameter, localised heating, powder metallurgy, strain path, titanium, upsetting

Date received: 28 January 2021; accepted: 9 May 2021

Introduction and background details

Plastic deformation is extensively engaged in the metal forming process for different applications. Preferably, components will be shaped to a permanent form as a final product by the forming process. But, sometimes metals will fail too early through ductile fracture due to the heterogeneity of the material. The mechanism of failure/damage in ductile materials happens because of nucleation, growth and coalescence of the voids. In the initial state, the material may consist of the matrix, particles and voids. Also, it represents the shape and size of the particles and voids. During the metal forming process, metal provides the failure site where fracture can nucleate in micro-voids form because of the existence of second phase particles and inclusions in the metal alloys. With increasing the deformation, the nucleation of failure will increase by the void growth. At some

stage of deformation, the contact of nearest voids causes void coalescence which ultimately directs to the formation of macro-crack and damage through the ductile failure.¹ In the industrial metal forming process, various types of defects are observed. The most common defects that occur in the upsetting are central burst and hot tears. The central burst occurs at the centre of the component and hot tears occur on the outer surface of the component.^{2–4}

¹Department of Mechanical Engineering, National Institute of Technology Warangal, Telangana, India

²Department of Mechanical Engineering, Karunya Institute of Technology and Sciences, Karunya Nagar, Coimbatore, India

Corresponding author:

R Tharmaraj, Institute of Fundamental Technological Research Polish Academy of Sciences, Pawińskiego 5B, 02-106 Warsaw, Poland.
Email: tharmaraj88@yahoo.com

These types of troubles have been approached by the engineer through more number practices and many experimental methods. But, the procedures consume more time and infrequently give the solution for finding the ductile fracture. The forecast of crack opening permits process alteration, which provides damage-free products with financial savings. The incidence of the fracture in the forming process has been analysed by different researchers.⁵⁻⁷ They found that the starting of nucleation happens in the beginning stage after that void growth happens because of the localised deformation. In the final, coalescence happens because of the necking in the localised areas.

The occurrence of damage is an important characteristic in the upsetting process which could be helpful for an industrial engineer to predict the damage limit of the components in various engineering applications such as aerospace, automobile, medical etc. Enhancing the damage limit of the material is a crucial plan in the metal forming process. In recent days, industries want to increase the damage limit of the components for different applications. Hence, many researchers have studied the improvement of the failure limit for various materials using different methods.⁸⁻¹⁰ Researchers have studied the workability of dual-phase steel at various heat treatments (HTs) process.⁸ They have analysed the forming limit of the components by conducting the compression test and observed that the strain to failure is different for different HTs due to change in microstructures. The author has investigated the various methods such as annealing (473 K–773 K) before forming and application of counter-pressure (100 MPa–300 MPa) during upsetting for the improvement of workability of AZ31B magnesium alloy.⁹ He found that the effect of annealing temperatures and the counter-pressure in the upsetting has a major effect on the workability of the material. He observed that the workability of the material has increased at a higher annealing temperature (773 K) and also by the application of counter-pressure ranging from 100 MPa to 200 MPa due to grain refinement during the upsetting. Authors have studied the effect of HT on the performance (properties and surface quality) of P/M cold work tool steel by adopting a new technique of HT.¹⁰ They find that due to fine microstructure, a changed, cracked and pore-free surface is found in the selected P/M tool steel. But, in the upsetting of porous specimens, the transmission of crack takes place in the equatorial zone because of the existence of triaxiality stress in the circumferential route and damage arises in the outer position because of the stresses and the pores.^{11,12} Therefore, the damage limit of the porous specimens relies on the stresses and the pores. So, such kind of stresses and pores must be removed to get a better damage limit of the components. Hence, it is compulsory to decrease the stresses and decrease the pores in the outer sites for improving the fracture limit. Thus, the analysis of the damage behaviour for

the porous specimens is a dynamic research area between the researchers during the process.

It is observed from the above literature that the damage limit of the workpiece relies on different factors. But, in the upsetting of porous specimens, stresses are accumulated in the outer zone and the inherent pores are more in this zone. Therefore, the damage happens in these positions and the fracture point could be decreased. Hence, it is essential to lessen the stresses and reduce the pore amount to improve the failure limit of the specimens. The above-mentioned researchers have not given attention to the relieving of stresses and the reduction of porosity level in the outer position of the components. Thus, the present work is aimed to identify the fracture location of the newly developed sintered porous aluminium-titanium preforms and to increase the damage limit of these specimens by applying the novel way of selective or localized heating in the outer or equatorial position of the compressed preform at different conditions (100 °C–250 °C) using different fracture criteria under triaxial condition. Heating the preforms selectively in the damage sites postponement the fracture and enhanced the damage limit.

Mathematical calculations

Different upsetting parameters based on stresses and strains were to be calculated under the triaxial condition for the measurement of the critical damage parameter (CDP) and the strain path analysis of different Al–Ti components.

Stress and strain relations

Based on this type, the following expressions are used to determine the CDP of P/M Al–Ti samples for various IRDs and various Ti compositions.¹³⁻¹⁶

$$\text{True axial stress } (\sigma_z) = \frac{F}{\pi \frac{(D_{tc} + D_{bc})^2}{4}} \quad (1)$$

$$\text{Hoop stress } (\sigma_\theta) = \left[\frac{(2\nu + R^2)}{2 - R^2 + 2R^2\nu} \right] \sigma_z \quad (2)$$

$$\text{Poisson's ratio } (\nu) = \frac{\ln \left[\frac{D_{tc} + D_{bc}}{2D} \right]}{2 \ln \left(\frac{H}{H_r} \right)} \quad (3)$$

$$\text{Mean stress } (\sigma_m) = \frac{\sigma_z + 2\sigma_\theta}{3} \quad (4)$$

$$\begin{aligned} \text{Effective stress } (\sigma_{\text{eff}}) \\ = \left[\frac{[\sigma_z^2 + 2\sigma_\theta^2 - R^2(\sigma_z\sigma_\theta + \sigma_\theta^2 + \sigma_z\sigma_\theta)]}{(2R^2 - 1)} \right]^{0.5} \end{aligned} \quad (5)$$

Based on strain type, the following expressions are used to determine the CDP of the newly developed porous Al–Ti samples.^{17–19}

$$\text{True axial strain } (\mathcal{E}_z) = \ln \left(\frac{H}{H_f} \right) \quad (6)$$

$$\text{Mean strain } (\varepsilon_m) = \frac{\mathcal{E}_z + 2\mathcal{E}_\theta}{3} \quad (7)$$

$$\text{Hoop strain } (\mathcal{E}_\theta) = \ln \left[\frac{2D_b^2 + \left(\frac{D_{tc} + D_{bc}}{2} \right)^2}{3D^2} \right] \quad (8)$$

$$\begin{aligned} \text{Effective strain } (\mathcal{E}_{\text{eff}}) &= \left\{ \left(\frac{2(2+R^2)}{3} \right) [2\mathcal{E}_\theta^2 + 2\mathcal{E}_z^2 + 4\mathcal{E}_z\mathcal{E}_\theta] \right. \\ &\quad \left. + \left[\left(\frac{(2\mathcal{E}_\theta - \mathcal{E}_z)^2}{3} \right) (1 - R^2) \right] \right\}^{0.5} \end{aligned} \quad (9)$$

where F is the upsetting load applied in the axial direction. D is the diameter of the porous Al–Ti components before the compression. The D is measured by using the vernier calliper. D_{tc} and D_{bc} is the contact diameter of the porous Al–Ti samples in the top and bottom portion after deformation. The D_{tc} and D_{bc} are measured by using the vernier calliper. D_b is the bulged diameter of the porous Al–Ti samples, measured by using the vernier calliper. R is the relative density (RD) of the porous Al–Ti samples, measured by using the Archimedes principle. ν is the Poisson's ratio, determined by using the equation (3). H is the initial height of the porous Al–Ti component before applying the load and H_f is the height of the deformed porous Al–Ti samples after applying the load. The H and H_f are measured by using the vernier calliper.

Damage criteria

The ductile fracture of P/M materials under various conditions of deformation depends on process parameters that influence the stresses and strains in cold working conditions. Many researchers have proposed various fracture criteria to find the ductile fracture.^{20–23} The detailed explanation is given below. All the fracture criteria are based on the macro mechanical approach in which failure occurs when the stresses and strains reach a critical value. As stated by these criteria, the workpiece loses its strength on compressing the specimens to higher values of strains and the value of strain at which fracture occurs is called critical damage. The value of the CDP will vary with the type of criteria is assumed.

The author has established the CDP expression for strain energy to fracture during the plastic deformation process.²⁰

$$C_1 = \int_0^{\bar{\mathcal{E}}_f} \bar{\sigma} \, d\bar{\mathcal{E}} \quad (10)$$

Researchers have introduced a mathematical formula for finding the CDP and they reported that damage occurs when tensile strain energy reaches a maximum critical value.²¹

$$C_2 = \int_0^{\bar{\mathcal{E}}_f} \sigma_1 \, d\bar{\mathcal{E}} \quad (11)$$

The authors have proposed the normalized version of the Cockcroft and Latham damage criterion.²² This criterion considered the important parameter for the ductile fracture as the ratio of maximum principal tensile stress to the effective stress and the CDP is expressed as

$$C_3 = \int_0^{\bar{\mathcal{E}}_f} \frac{\sigma_1}{\bar{\sigma}} \, d\bar{\mathcal{E}} \quad (12)$$

Researchers have introduced the ductile fracture model with considering the CDP as the ratio of mean stress to effective stress.²³

$$C_4 = \int_0^{\bar{\mathcal{E}}_f} \frac{\sigma_m}{\bar{\sigma}} \, d\bar{\mathcal{E}} \quad (13)$$

where $\bar{\sigma}$ is the effective stress, $d\bar{\mathcal{E}}$ is the effective strain increment, $\bar{\mathcal{E}}_f$ is the effective strain at fracture, σ_z is true axial stress, σ_θ is true hoop stress, σ_1 is the maximum principal stress. $\sigma_1 = \sigma_\theta$ for axisymmetric cylindrical compression test.²⁴ C_1 , C_2 , C_3 and C_4 are the CDP of porous Al–Ti samples. Substitute the stress and strain relation in equation (10) to (13), the CDP is calculated.

Experimental procedures

Material selection

The components were obtained from the aluminium (Al) and titanium (Ti) elements, which were developed via the atomization route and were in the form of powders, to investigate the fracture characteristics of porous Al–Ti samples. Because of its beneficial properties, the combination of these materials (Al and Ti) has been commonly used in the automotive and aerospace industries.^{25–28} Hence, this analysis aims to focus on a subset of these (Al and Ti) specimens and assess their response to damage characteristics under various localized heating conditions.

Because of its advantages in economic, specific and captive applications used in various industries such as aerospace and automobile, the samples were produced using the powder metallurgy (P/M) technique.²⁹ The Al and Ti particles come from the SRL Company in Maharashtra, India, and have an average size of 44 μm and 74 μm , respectively. Both particles are 99.5 percentage pure, with just 0.5 percentage insoluble impurities. The scanning electron microscope (SEM) representation of the Al and Ti powder particles is shown in Figure 1(a) and (b). TESCAN and VEGA 3 LMU are the labels and versions of the SEM equipment. The irregular shape is found in the Al particles in Figure 1(a) and the spherical shape is found in the Ti particles in Figure 1(b). To achieve a homogeneous powder blend, the correct amount of powders are taken and blended in the porcelain bowl for 45 to 60 minutes by manually stirring.³⁰ Using the X-ray diffraction (XRD) instrument, the received powder particles are also analysed to confirm the presence of Al and Ti particles in the powder. PANalytical and X'Pert Powder XRD is the make and model of the XRD equipment. Figure 1(c) displays the XRD picture of the Al and Ti

powder particles and shows that the particles (Al and Ti) are present in the obtained powders.

Compacts preparation

By compressing/compacting the mixed Al and Ti powders, the necessary dimension of the porous Al–Ti components was prepared from the powder particles. The compaction is taken place by pouring the correct amount of powders into the proper die tools with the help of a hydraulic press machine (HPM). The maximum capacity of the HPM is 0.5 MN and the HPM is made by SVS Hydraulics from Hyderabad, India. The obtained geometry of the prepared samples is 10 mm in height and 10 mm in diameter. The application of compaction pressure for choosing the initial relative densities (IRDs) (80%, 85% and 90%) for different weight percentages of Ti (2%, 4% and 6%) in the Al component is 318 MPa to 420 MPa. With increasing the amounts of Ti contents in the Al, intermetallic compounds (Ti_3Al , TiAl and TiAl_3) will be formed. But, this research focuses on only Ti particles in the Al matrix. Hence, the least quantity of Ti contents at

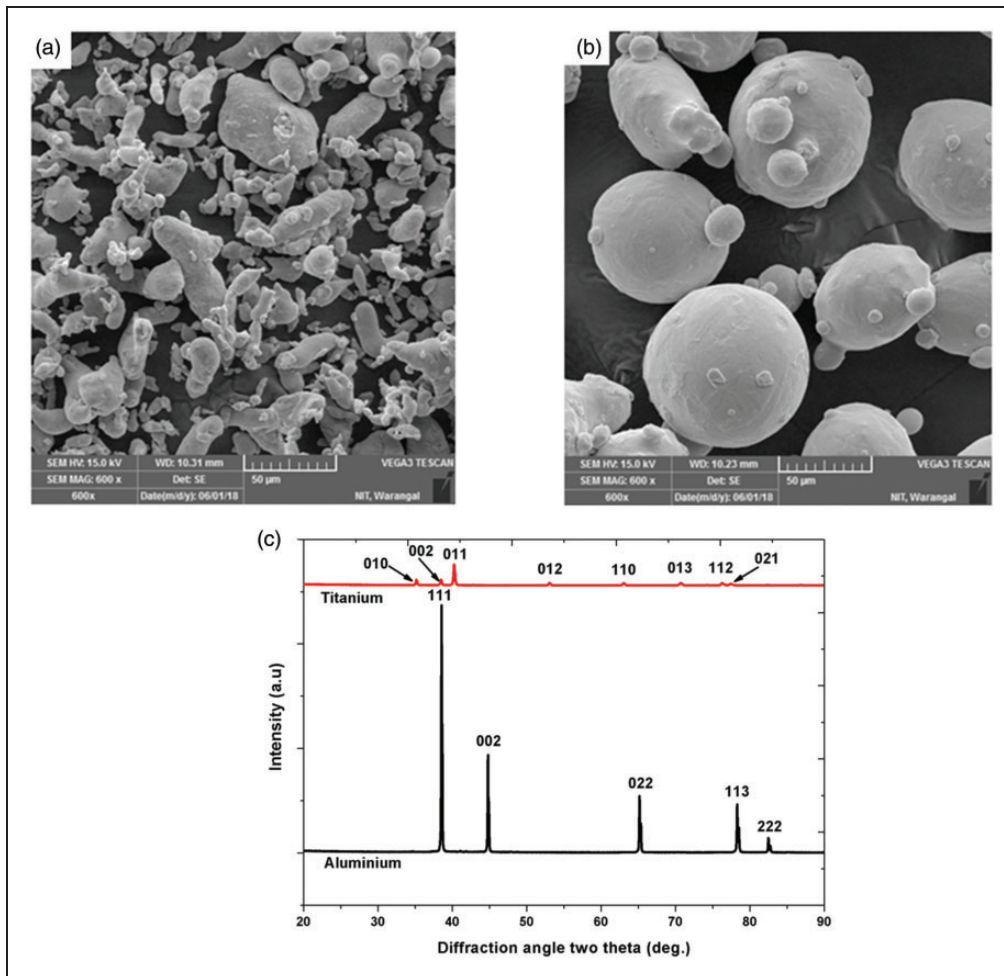


Figure 1. (a) SEM picture of Al powder particle, (b) SEM picture of Ti powder particle, and (c) XRD plot of Al and Ti powder particles.

an equal difference (2%, 4% and 6%) was selected. In compaction, friction may take place between the particles and the die parts which could affect the quality of the compacts as well as the life of the die parts. So, zinc stearate was used as a lubricant on the die tools to avoid friction. Then, the prepared compacts are sintered in standard ambient pressure at the temperature of $550 \pm 10^\circ\text{C}$ for 1 h holding time using the electrical muffle furnace. The furnace is made by Swam Equip from Tamilnadu, India. After the sintering process, the dispersion of Ti in the samples is analysed using the SEM equipment and the image is shown in Figure 2(a) to (c). It is noticed from Figure 2 that the Ti elements are dispersed uniformly in the components. Also, the presence of Al and Ti components in the prepared sintered Al-Ti samples are analysed using the XRD equipment and the image is shown in Figure 2(d) and confirmed that Al and Ti

components are present in the newly developed preforms.

Localised heating in the upsetting test

Here, a method of selective or localised heating (SH) is introduced in the outer or equatorial sites of deformed porous Al-Ti samples to investigate the fracture characteristics at various IRDs for different Ti compositions under different temperatures. In this SH method, the initial height, diameter and the IRD of the samples were noted before applying the compression load. With the incremental deformation load, the upsetting was performed on the newly developed P/M Al-Ti samples using the HPM at room temperature (27°C) at the same strain rate (0.1 s^{-1}). By the application of forging load, the porous work-piece is deformed into the different amount of strains.

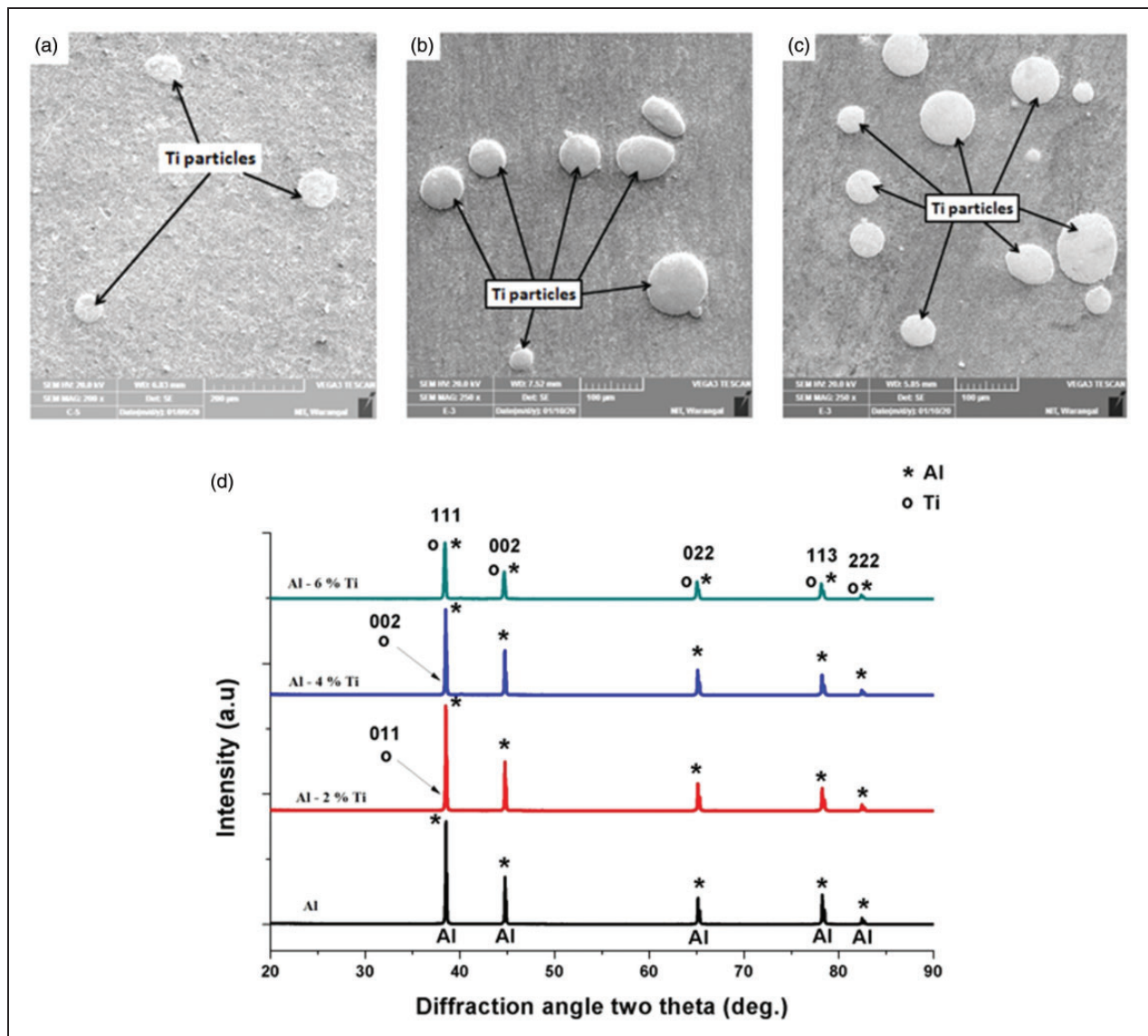


Figure 2. (a) SEM picture of sintered porous Al – 2% Ti samples, (b) SEM picture of sintered porous Al – 4% Ti samples, (c) SEM picture of sintered porous Al – 6% Ti samples, and (d) XRD plot of sintered Al and Al-Ti samples.

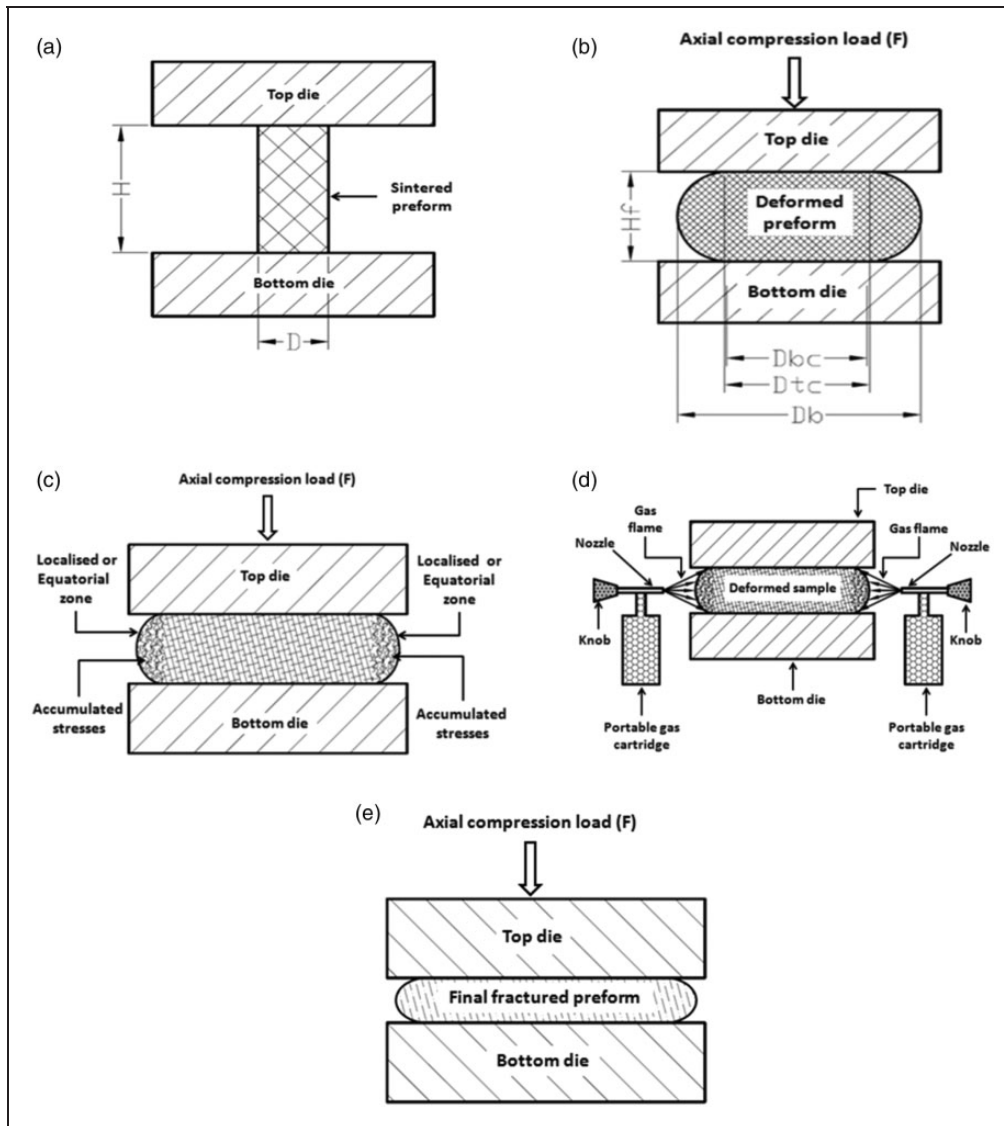


Figure 3. The schematic diagram for conducting the SH upsetting test: (a) application of deformation load on the sintered specimen, (b) specimen is deformed after the application of load, (c) stresses accumulated in the equatorial position of the deformed sample, (d) adopting the SH technique in the outer region of the deformed sample and (e) application of load on the deformed samples after the SH.

The complete schematic diagram for describing the SH technique is given in Figure 3(a) to (e). In the beginning, the porous Al–Ti samples are located in between the dies (top and bottom) which are attached with the HPM as seen in Figure 3(a). The deformation test is performed on the developed porous Al–Ti components by giving the deformation load (F) incrementally and their representation is given in Figure 3(b). After every incremental deformation, the dimensions of the samples (diameter and height) and the RDs are changed. The changed dimensions and the RD after the deformation are noted for analysing the failure parameter of the samples. The stresses and the pores are more in the outer zone of the components during the compression.^{11,12} The diagram for describing the stresses and the pores is given in Figure 3(c). These two factors have an impact on

the damage limit of the material. Hence, it is compulsory to decrease the stresses and the pores in the outer position. The stresses and pores are relieved by adopting the SH technique in the equatorial zone of the P/M samples. The schematic diagram of the SH method is given in Figure 3(d) and noticed that the SH is applied to the compressed samples in the equatorial zones at which the failure happens with the aid of a portable gas cartridge. The temperatures of the samples were noted by the infrared thermometer and the observed values are 100 °C, 140 °C, 195 °C, 220 °C and 250 °C. Once, the SH is completed on the outer position of the deformed specimen, again the deformation is performed on the corresponding selective heated specimen as seen in Figure 3(e). The upsetting was stopped after the damage happens on the outer face of the workpiece.

Results and discussion

Evolution of strain paths for different weight percentages of Ti at different SH conditions

The strain paths of newly developed porous Al-Ti samples for different weight percentages of Ti (2%–6%) and various IRDs (80%–90%) under different SH conditions (100 °C–250 °C) was analysed. Figure 4(a) to (c) gives the typical experimental strain paths of P/M Al-Ti samples with the IRD of 90% for different compositions of Ti (2%–6%) under various SH conditions (100 °C–250 °C). The value of hoop strain (HS) is more in the circumferential direction with the raise in the true axial strain (TAS) irrespective of the SH and the compositions of Ti contents. It is found that the strain paths of Al-Ti samples differ with the SH and the weight percentages of Ti compounds in the developed P/M samples. It is observed from Figure 4(a) that the distance between the two points in the strain paths has improved with the higher SH conditions concerning TAS. This is because of the

samples flow behaviour and the densification of the components. The flow behaviour of P/M Al-Ti samples has increased towards the outer zone with the higher heating conditions (250 °C) due to the reduction in the stresses in the outer zones. Therefore, the failure strain has improved for the higher level of SH condition. Also, the RD of the porous Al-Ti samples has improved at a superior SH temperature (250 °C) than other SH conditions because of the reduction in the amount of porosity.^{31,32} The amount of porosity for the newly developed porous Al-Ti samples was determined using the formula porosity = $\frac{\text{Volume of void}}{\text{Volume of Al-Ti composite}}$. The volume of Al-Ti composite ($V_{\text{Al-Ti}}$) is calculated by the Archimedes principle using the weight balance machine. Void volume (V_v) of deformed Al-Ti composite is calculated using the formula, $V_v = \frac{\rho_{\text{the,Al-Ti}} - \rho_{\text{exp,Al-Ti}}}{\rho_{\text{the,Al-Ti}}}$. Where, $\rho_{\text{the,Al-Ti}}$ is the theoretical density of P/M Al-Ti preforms and $\rho_{\text{exp,Al-Ti}}$ is the experimental density of deformed P/M Al-Ti preforms. The experimental density of deformed powder metallurgy Al-Ti preforms

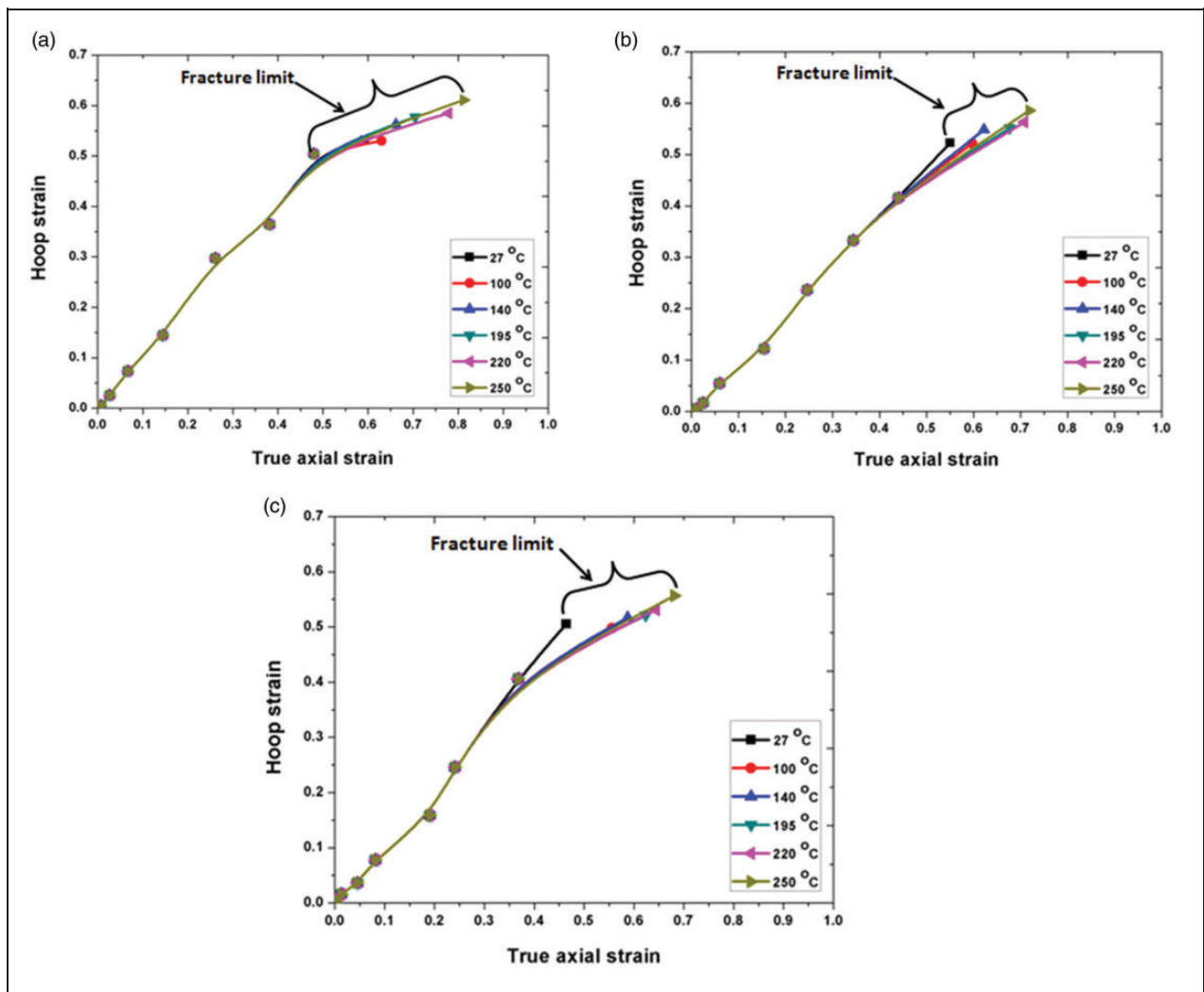


Figure 4. Role of SH on the strain paths of P/M Al-Ti samples for various weight percentages of Ti: (a) 2% Ti, (b) 4% Ti, and (c) 6% Ti.

($\rho_{\text{exp,Al-Ti}}$) is determined by the Archimedes principle using the weight balance machine. The theoretical density of Al-4% Ti composite ($\rho_{\text{the,Al-Ti}}$) is calculated using the formula $\frac{100}{\rho_{\text{the,Al-Ti}}} = \left(\frac{\text{Wt.}\% \text{ of Al}}{\rho_{\text{the,Al}}} + \frac{\text{Wt.}\% \text{ of Ti}}{\rho_{\text{the,Ti}}} \right)$. Theoretical density of Al ($\rho_{\text{the,Al}}$) is 2.7 g/cm³ and the theoretical density of Ti is 4.506 g/cm³. The porosity results of deformed Al-Ti samples for different SH are listed in Supplemental Table 1. It is observed from Supplemental Table 1 that the levels of porosity have reduced with the higher SH conditions (250 °C). Hence, the void nucleation (VN) is less for samples with a higher level of SH (250 °C) and the VN is more for samples with the lower SH conditions (100 °C). Therefore, a higher failure strain is obtained at higher SH irrespective of the Ti contents. Also, it is found that the strain path moves downward with the higher contents Ti particles in the P/M samples irrespective of SH conditions because of the influence of pores. The flow behaviour of the P/M samples is obstructed by the addition of reinforcements in the samples.^{31,33,34} Therefore, the failure strain has reduced for more amounts of Ti

contents in the workpiece. Also, the amount of porosity has increased with the rise in the compositions of Ti contents which could reduce the densification of the samples.^{31,34} Hence, the VN is more for samples with the higher amounts of Ti contents and the VN is less for the lower contents of Ti particles. Therefore, a higher failure strain is obtained for 2% of Ti components irrespective of the SH conditions. The same kind of results is obtained in the case of TAS vs effective strain (ES) plot for different Ti compositions (2%–6%) at various SH conditions (100 °C–250 °C) as shown in Figure 5(a) to (c).

Evolution of strain paths for various IRDs at different SH conditions

The strain paths of porous Al-Ti samples for different IRDs (80%–90%) and different Ti contents (2%–6%) under different SH conditions (100 °C–250 °C) was analysed. Figure 6(a) to (c) gives the typical experimental strain paths of porous Al-4% Ti samples with various IRDs (80%, 85% and 90%) at different SH conditions (100 °C–250 °C). The results of HS is more in the circumferential direction with an

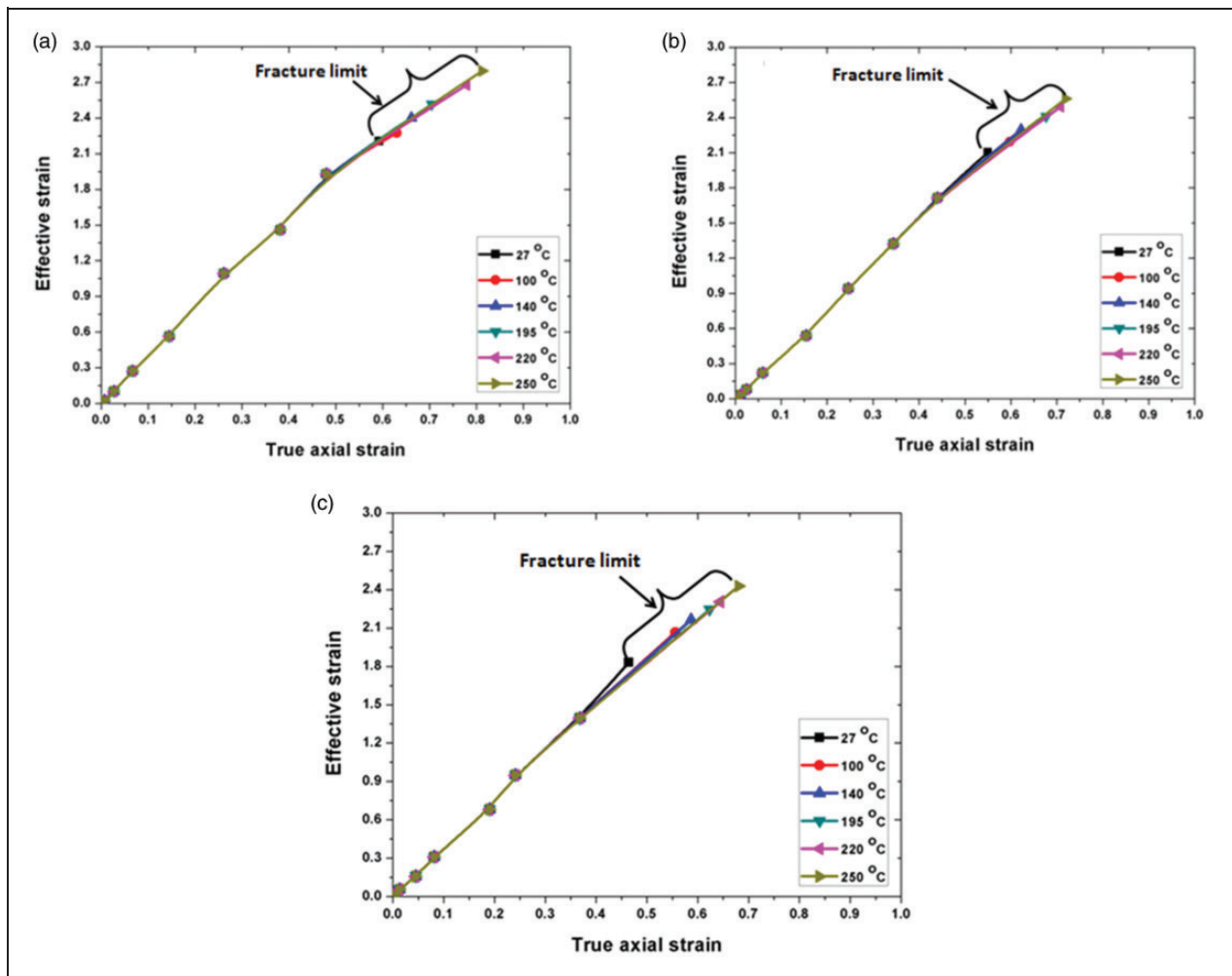


Figure 5. Role of SH on the ES concerning TAS of P/M Al-Ti samples for various weight percentages of Ti: (a) 2% Ti, (b) 4% Ti, and (c) 6% Ti.

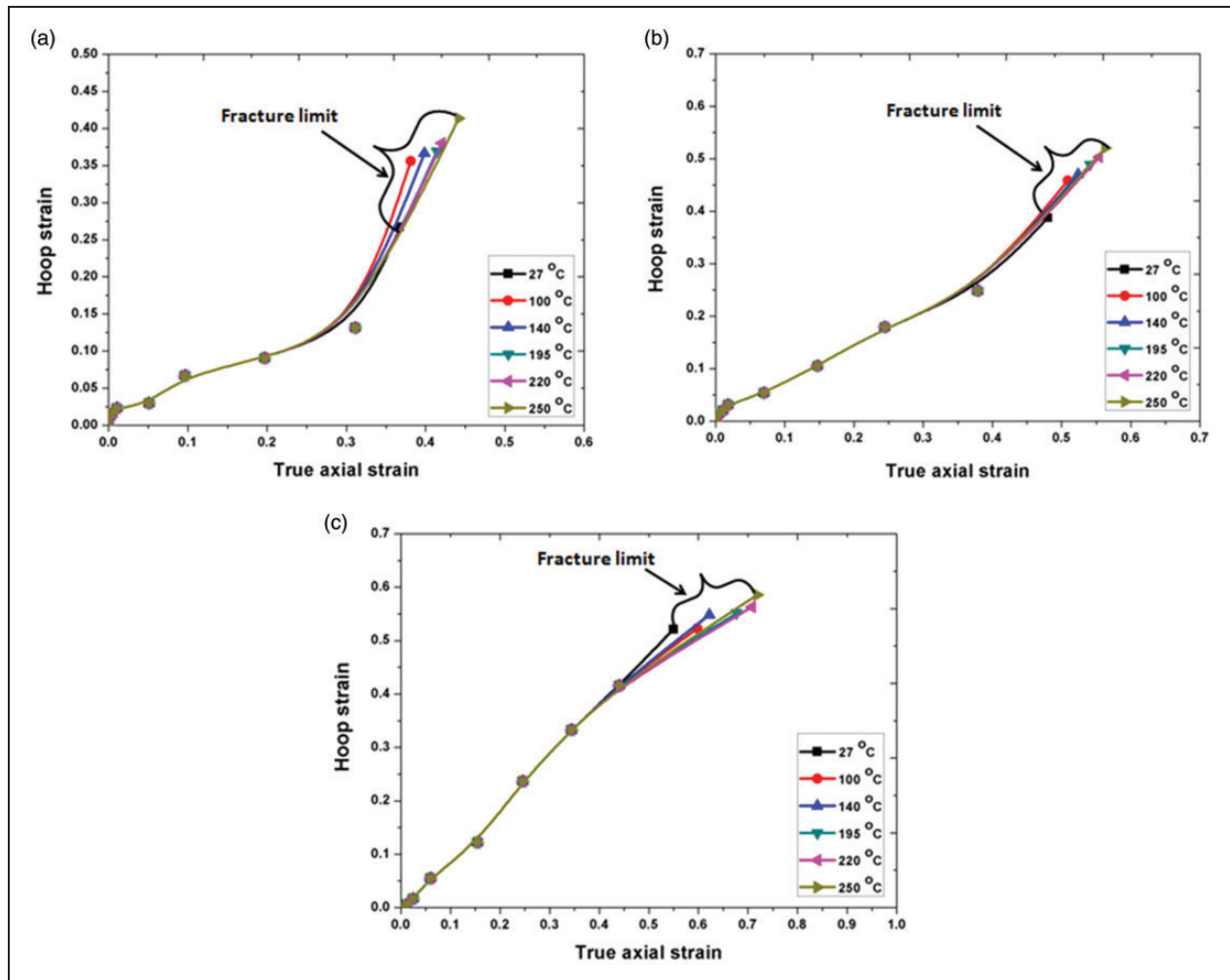


Figure 6. Role of SH on the strain paths of porous Al – 4% Ti components for various IRDs: (a) 80%, (b) 85%, and (c) 90%.

increase in the TAS irrespective of the SH and the IRDs. It is found that the strain paths of P/M Al-4% Ti samples vary with the SH conditions and the preforms IRDs. It is observed from Figure 6(a) that the distance between the two points in the strain paths has improved with the higher SH conditions concerning TAS. This is because of the densification during the process. During upsetting, the closure of pores has improved with the higher heating conditions (250 °C) which will increase the densification of the samples.^{31,32} For sample with the higher densification, the preforms flow behaviour has increased and hence the failure strain of the component is improved due to the reduction in the porosity.^{31–34} The amount of porosity for the porous Al – 4% Ti samples for various IRDs was determined and the results are given in Supplemental Table 2. It is observed from Supplemental Table 2 that the levels of porosity have reduced with the higher SH conditions (250 °C). Hence, the VN is less for samples with a higher level of SH (250 °C) and the VN is more for samples with the lower SH conditions (100 °C). Therefore, a higher failure strain is obtained at higher SH temperature. Moreover, it is found from

Figure 6 that the strain path moves upward with the higher value of IRD because of the amount of porosity. In the higher IRD, the level of porosity has reduced which will increase the densification and the materials flow behaviour.³⁴ Therefore, the failure strain has increased for the higher IRDs. Hence, the VN is less for the samples with the higher IRD and the VN is more for the lower value of IRD. Therefore, a higher failure strain is obtained for the higher IRD (90%) at the higher SH conditions (250 °C). The same kind of results is obtained in the case of TAS vs ES plot for different IRDs (80%–90%) at various SH conditions (100 °C–250 °C) as shown in Figure 7(a) to (c).

Analysis of CDP for different weight percentages of Ti at different SH conditions

In the forming process, the value of CDP is an essential variable to investigate the ductile fracture of the workpiece. The high value of CDP gives good formability and the low value of CDP gives poor formability. But, this CDP differs by various process parameters such as materials compositions, IRD

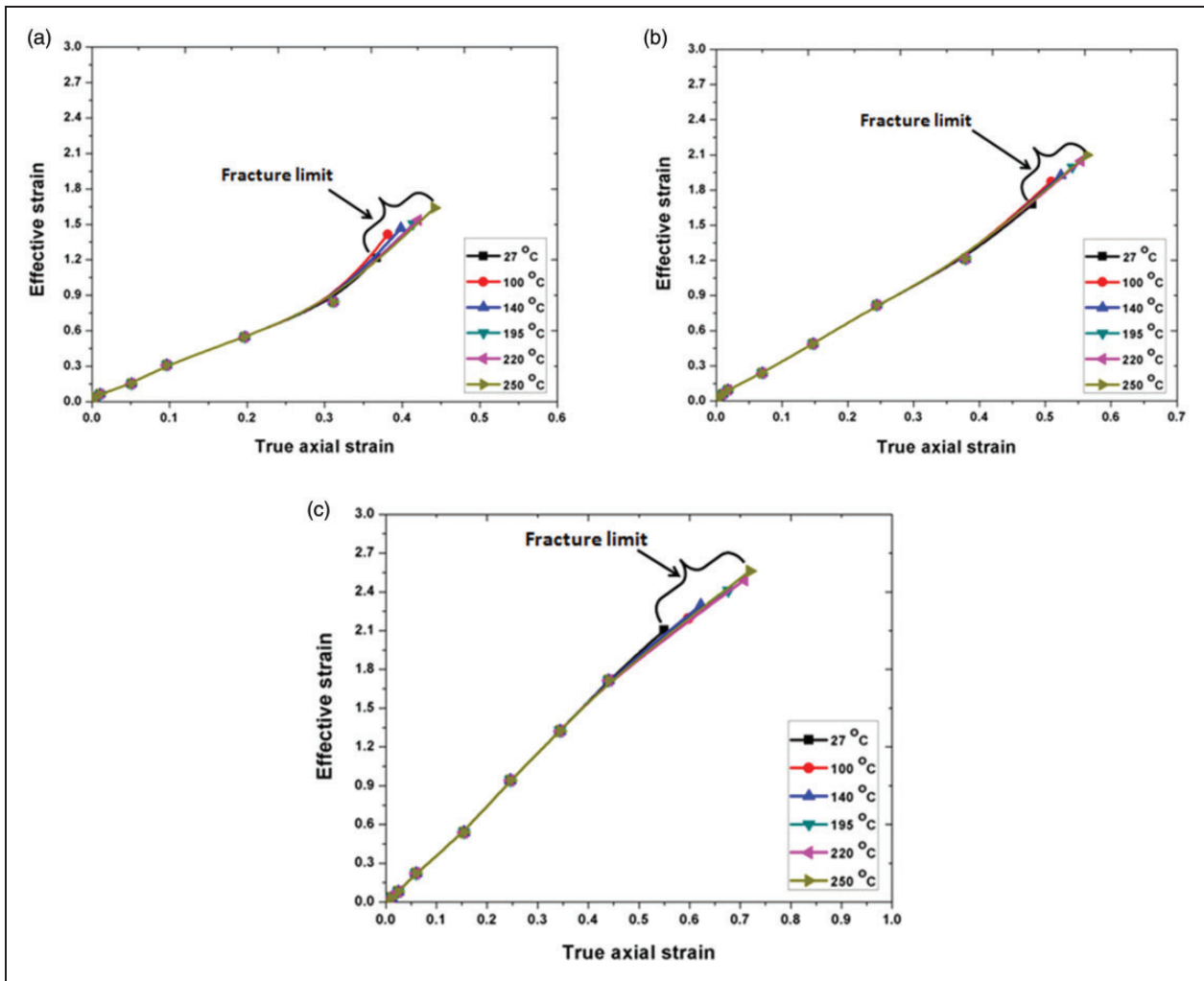


Figure 7. Role of SH on the ES concerning TAS of porous Al – 4% Ti components for various IRDs: (a) 80%, (b) 85%, and (c) 90%.

and temperature. So, it is a need to increase the CDP of porous Al–Ti preforms which would be useful for engineering applications. Hence, in this present work, a novel method of SH is introduced at the damage site of the deformed specimens to enhance the CDP during the upsetting process using various fracture criteria. The CDP of porous Al–Ti components for various weight percentages of Ti (2%–6%) and different IRDs (80%–90%) under different SH conditions (100 °C–250 °C) was evaluated using different fracture criteria. Figure 8(a) to (d) gives the CDP plots of porous Al–Ti samples with the IRD of 90% for various weight percentages of Ti (2%–6%) under various SH conditions (100 °C–250 °C). It is noticed from Figure 8 that the weight percentage of Ti particles and the SH conditions are a superior response to the CDP of the developed P/M Al–Ti samples. It is observed from Figure 8 that the CDP of the samples has improved with the higher SH conditions. This is because of the relieving of stresses and the reduction of pores in the outer positions. In the compression of porous samples, the presence of stresses and the pores

are more in the equatorial sites of the specimens.^{11,12} These stresses and the pores are the major factors on the CDP of the workpiece. By the application of SH in the equatorial position, the amount of stresses and the pores has reduced and therefore the failure strain (effective strain) has enhanced due to the materials flow softening and the reduction in the porosity.^{31,32} So that the VN has been delayed and the CDP of the material has improved. The reduction of stress and the pore amount varies with variations in the SH conditions. For a higher SH condition (250 °C), the relieving rate of stress and pores is more and the relieving rate of stress and pore is low for the lower SH condition (100 °C). Hence, the effective strain has increased for the samples with the higher SH conditions and the value of effective strain has reduced for the samples with the lower SH condition. Thus, the CDP is more for the higher SH due to the slow VN and the CDP is low for the lower SH due to the faster VN. Moreover, it is found from Figure 8 that the CDP of porous Al–Ti samples has reduced with the higher contents Ti particles in the P/M samples

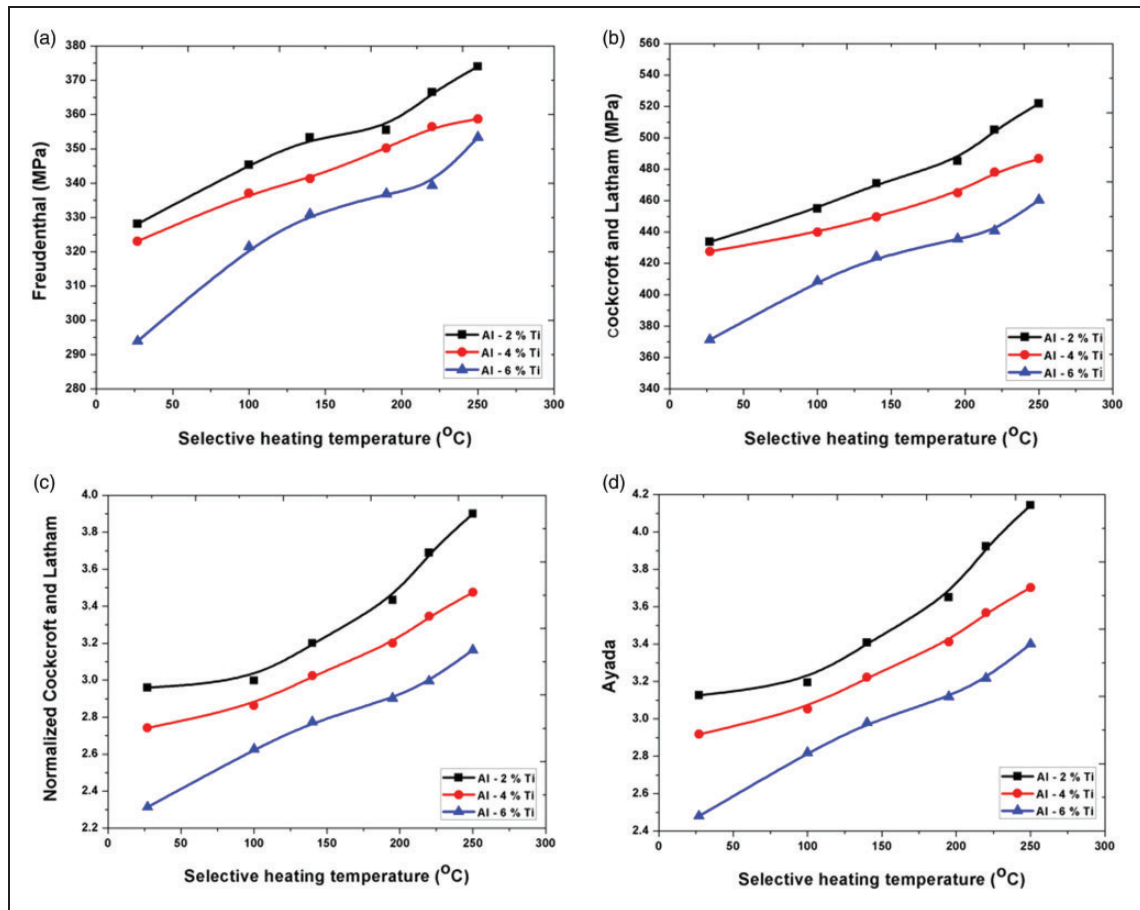


Figure 8. Role of SH on the CDP of P/M Al-Ti samples for different compositions of Ti under various fracture criteria.

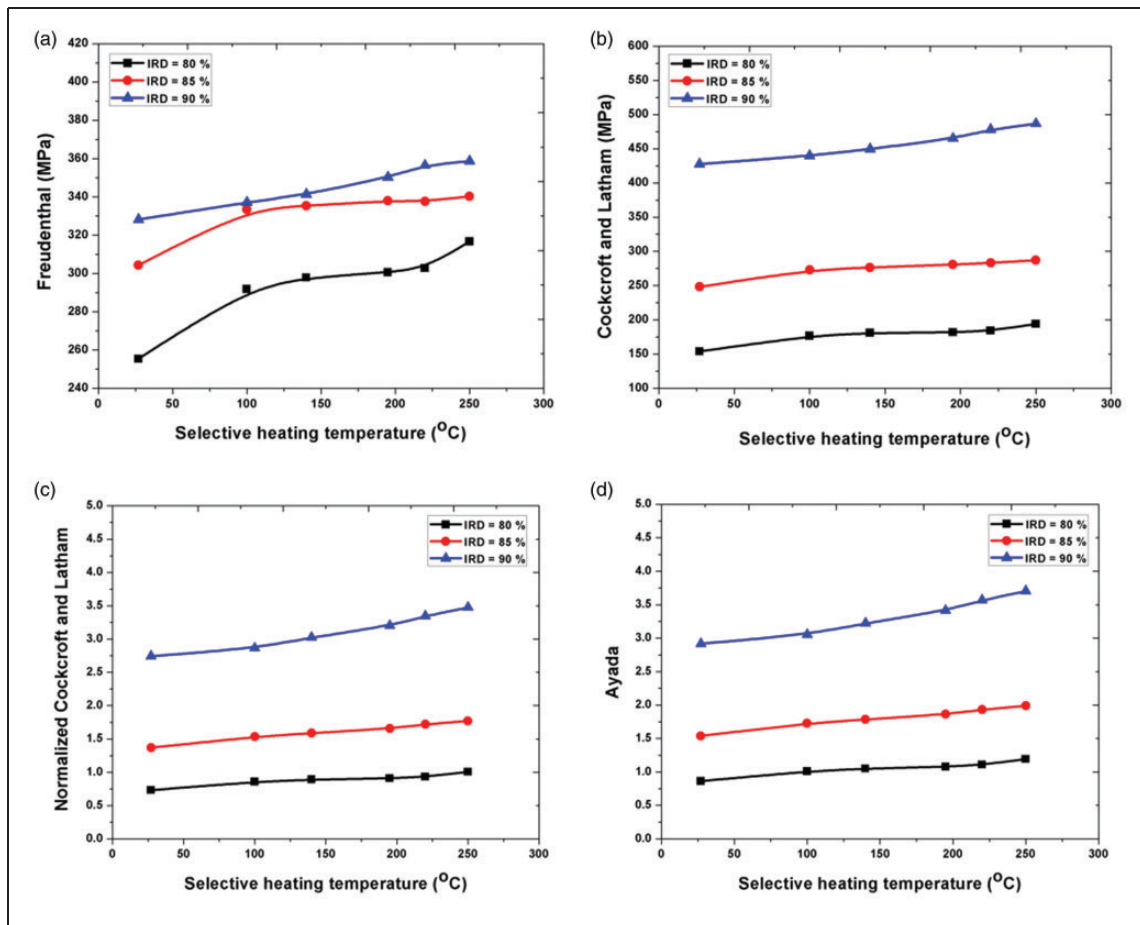


Figure 9. Role of SH on the CDP of porous Al-4% Ti samples for various IRDs under different fracture criteria.

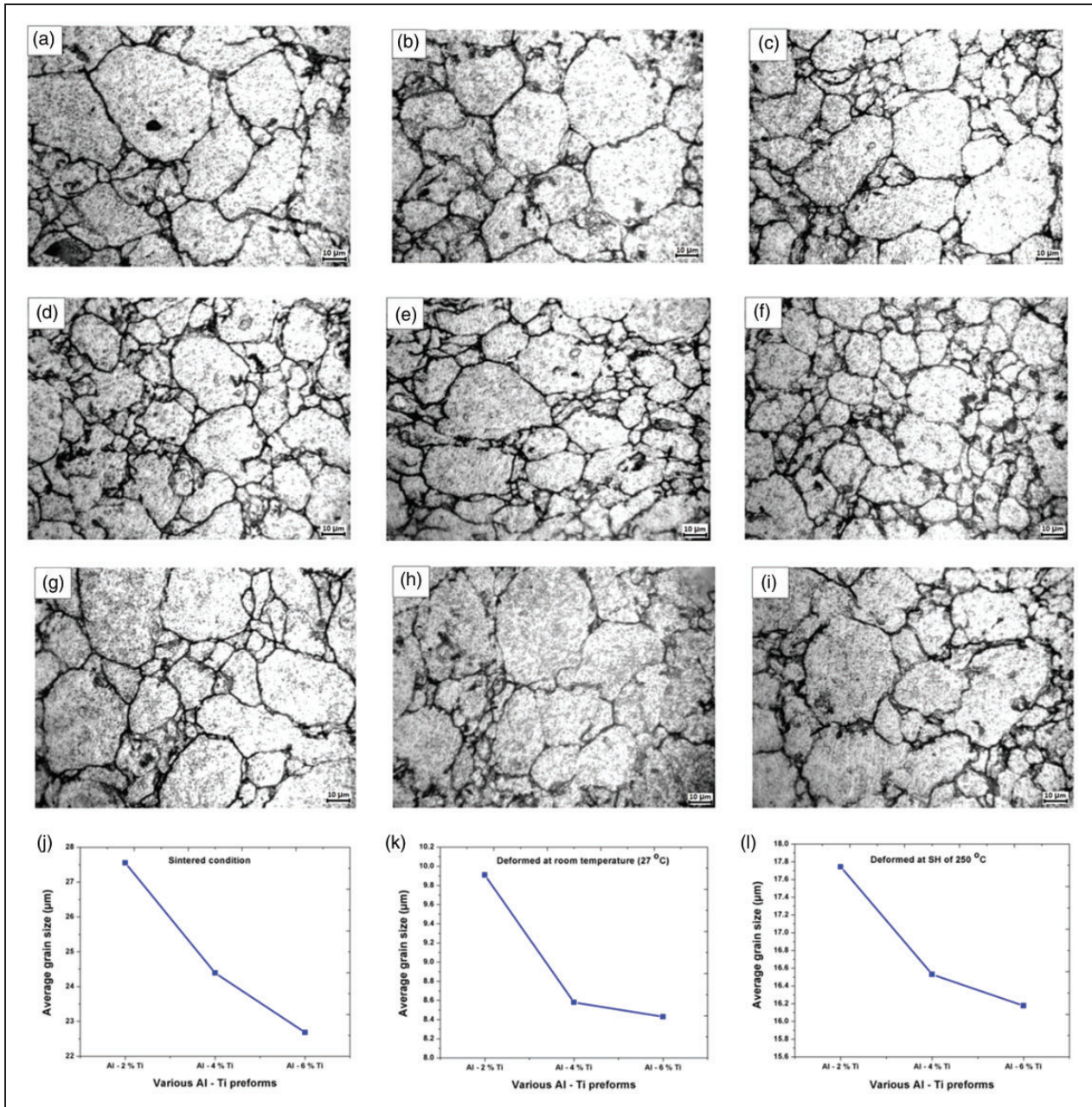


Figure 10. Microstructure and grain size of P/M Al-Ti samples at various conditions: (a) OM image of sintered Al – 2% Ti, (b) OM image of sintered Al – 4% Ti, (c) OM image of sintered Al – 6% Ti, (d) OM image of deformed Al – 2% Ti at 27°C, (e) OM image of deformed Al – 4% Ti at 27°C, (f) OM image of deformed Al – 6% Ti at 27°C, (g) OM image of deformed Al – 2% Ti at 250°C, (h) OM image of deformed Al – 4% Ti at 250°C, (i) OM image of deformed Al – 6% Ti at 250°C, (j) grain size of sintered Al-Ti samples, (k) grain size of deformed Al-Ti samples at 27°C, and (l) grain size of deformed Al-Ti samples at 250°C.

irrespective of SH conditions because of the pores. The amount of porosity has increased with the rise in the compositions of Ti contents which could reduce the RD and the flow behaviour of the samples.³⁴ Therefore, the effective strain of the sample has reduced due to the larger amounts of pores. Hence, the VN in the sample has been increased and the CDP of the material has reduced. Thus, the CDP is less for samples with the higher amounts of Ti contents (6%) due to faster VN and the CDP is more for samples with the lower amounts of Ti contents (2%) due to

slow VN. Therefore, the maximum value of CDP is achieved in the 2% of Ti at the largest value of SH condition (250°C).

Analysis of CDP for various IRDs at different SH conditions

The CDP of porous Al-Ti samples for various weight percentages of Ti (2%–6%) and different IRDs (80%–90%) under different SH conditions (100°C–250°C) was evaluated using different fracture criteria.

Figure 9(a) to (d) gives the CDP plots of porous Al–4% Ti samples with different IRDs (80%–90%) under different SH conditions (100 °C–250 °C). It is observed from Figure 9 that the CDP has enhanced for the samples with the higher IRD due to less amount of porosity for any SH conditions. Therefore, the RD of the sample has increased which yields to increase in the flow behaviour of the samples.^{31–34} Hence, the effective strain at failure is improved due to the reduction of porosity. Therefore, the VN in the Al–Ti sample is slow for the higher value of IRD (90%) which increase the CDP of the material during the process. On the other side, the CDP value has decreased for the samples with the low value of IRD due to the larger amounts of pores. Hence, the flow behaviour of the sample has reduced due to the lower densification.^{31–34} Therefore, the effective strain of the sample has reduced because of the higher amount of porosity. Thus, the VN in the sample has increased and the CDP of the sample has reduced. Moreover, the CDP has enhanced with the higher levels of SH for any IRDs due to the relieving of stresses and the closure of pores. Therefore, the maximum value of CDP is achieved in the higher IRD (90%) at the largest value of SH condition (250 °C).

Analysis of microstructures

The analysis of microstructures was carried out using the optical microscope (OM) for various Ti contents (2%–6%) and various IRDs (80%–90%) at various heating conditions (100 °C–250 °C). Initially, the porous Al–Ti samples were polished into a good finish using various kinds of polishing methods such as paper polishing and cloth polishing. After that, the polished samples were undergone to the microstructure evolution using the OM instrument. The model of the OM is Quasmo ISI Microscope and the software used in the OM is Quasmo iview 3.7. The etchant and the time for etching the sample are chosen as Keller type and 60–70 s. Figure 10(a) to (l) gives the optical microstructures and grain size (GS) of sintered and deformed P/M Al–Ti samples for various Ti contents (2%–6%). It is noticed from Figure 10 that the entire P/M sample consists of equiaxed grain size in the sintered conditions (seen in Figure 10(a) to (c)). The influence of Ti contents (2%–6%) and the IRDs (80%–90%) on the optical image of compressed porous Al–Ti specimens was studied at various SH conditions (100 °C–250 °C) using the OM. Figure 10 (d) to (i) show the microstructure of compressed porous Al–Ti specimens with an IRD of 90% for different weight percentages of Ti contents (2%–6%) at room (27 °C) and SH of 250 °C. The Ti contents play a significant role in the microstructure of P/M preforms for all processing conditions during the upsetting tests. It is found that the GS of the sample has increased (seen in Figure 10(k) and (l)) for the higher

SH conditions (250 °C) due to the growth of the grains.^{35,36}

Conclusions

The CDP of the porous Al–Ti samples for various weight percentages of Ti (2%–6%) and different IRDs (80%–90%) have been analyzed by adopting the novel technique of SH under various temperatures (100 °C–250 °C). Following are the major conclusions.

- SH technique is the right route to improve the CDP of the porous samples by reducing the stresses accumulated in the equatorial position and minimizing the pores in the equatorial position during the upsetting.
- Strain paths of various porous Al–Ti specimens have been investigated for different Ti contents and various IRDs under various SH conditions. The results showed that the fracture strain of the specimens has enhanced for the higher value of SH and the higher value of IRD due to the reduction of stresses and the amounts of porosity. Also, the fracture strain has decreased for samples with the higher contents of Ti particles due to the more amount of porosity.
- CDP of various porous Al–Ti specimens have been analysed using different damage criteria and found that the CTD has improved for the higher SH conditions and the higher IRD due to the reduction of pores which yield a slow VN. Also, the CDP has decreased for samples with the higher contents of Ti particles due to the more amount of porosity which provides the faster VN.
- Microstructure evolution of selective heated porous Al–Ti specimens was analysed using the OM equipment at various processing conditions during the upsetting. Heating selectively at the equatorial site of the P/M components affects the GS. The GS has increased for the higher SH conditions due to the growth of the grains and the CDP of the material was enhanced due to this.

Author's note

R Tharmaraj is now affiliated with Institute of Fundamental Technological Research Polish Academy of Sciences, Pawińskiego 5B, 02-106 Warsaw, Poland.

Declaration of conflicting interests

The author(s) declared no potential conflicts of interest with respect to the research, authorship, and/or publication of this article.

Funding

The author(s) disclosed receipt of the following financial support for the research, authorship, and/or publication of this article: The authors gratefully acknowledge the financial support of this work by the Department of

Science and Technology, New Delhi, Government of India under INSPIRE program (Vide Letter No.: DST/INSPIRE Fellowship/2016/IF160525).

ORCID iDs

R Tharmaraj  <https://orcid.org/0000-0001-6494-7664>

M Joseph Davidson  <https://orcid.org/0000-0003-0160-7368>

Supplemental material

Supplemental material for this article is available online.

References

- Chen ZT. *The role of heterogeneous particle distribution in the prediction of ductile fracture*. PhD Thesis. University of Waterloo, Canada, 2004.
- Johnson W and Mamalis AG. A survey of some physical defects arising in metal working processes. In: *Proceeding of the seventeenth international machine tool design and research conference*, Birmingham, 20–24 September 1976, pp. 607–621.
- Mamalis AG and Johnson W. Defects in the processing of metals and composites. *Stud Appl Mech* 1987; 15: 231–250.
- Johnson W. Manufacturing defects studies noting some of the early ideas of Robert Mallett (1810–1881). Irish engineer-scientist. *J Mater Process Technol* 1991; 26: 97–116.
- Thomason PF. Tensile plastic instability and ductile fracture criteria in uniaxial compression tests. *Int J Mech Sci* 1969; 11: 187–194.
- Kuhn HA and Lee PW. Strain instability and fracture at the surface of upset cylinders. *Metall Mater Trans B* 1971; 2: 3197–3202.
- Kobayashi S. Deformation characteristics and ductile fracture of 1040 steel in simple upsetting of solid cylinders and rings. *J Eng Ind* 1970; 92: 391–398.
- Park KS, Park KT, Lee DL, et al. Effect of heat treatment path on the cold formability of drawn dual-phase steels. *Mater Sci Eng A* 2007; 449–451: 1135–1138.
- Matsumoto R. Ductility improvement methods for commercial AZ31B magnesium alloy in cold forging. *Trans Nonferrous Met Soc China* 2010; 20: 1275–1281.
- Sturm R, Stefanikova M and Petrovi DS. Influence of pre heating on the surface modification of powder metallurgy processed cold work tool steel during laser surface melting. *Appl Surf Sci* 2015; 325: 203–210.
- Al-Mousawi MM, Daragheh AM, Ghosh SK, et al. Physical defects in metal forming processes and creation of a data base. *J Mater Process Technol* 1992; 32: 461–470.
- Rajeshkannan A and Narayan S. Strain hardening behaviour in sintered Fe–0.8% C –1.0% Si–0.8% Cu powder metallurgy preform during cold upsetting. *Proc IMechE, Part B: J Engineering Manufacture* 2009; 223: 1567–1574.
- Selvakumar N and Narayanasamy R. Deformation behavior of cold upset forming of sintered Al–Fe composite preforms. *J Eng Mater Technol* 2005; 127: 251–256.
- Mohan Raj AP, Selvakumar N, Narayanasamy R, et al. Experimental investigation on workability and strain hardening behaviour of Fe–C–Mn sintered composites with different percentage of carbon and manganese content. *Mater Des* 2013; 49: 791–801.
- Narayanasamy R and Ponalagusamy R. Unpublished report on P/M forging part-I. National Institute of Technology, Tiruchirappalli, Tamil Nadu, India, 2003.
- Doraivelu SM, Gegel HL, Gunasekera JS, et al. A new yield function for compressible P/M materials. *Int J Mech Sci* 1984; 26: 527–535.
- Narayanasamy R, Ramesh T and Pandey KS. Some aspects on workability of aluminium–iron powder metallurgy composite during cold upsetting. *Mater Sci Eng A* 2005; 391: 418–426.
- Narayanasamy R and Sathiya Narayanan C. Some aspects on fracture limit diagram developed for different steel sheets. *Mater Sci Eng A* 2006; 417: 197–224.
- Narayanasamy R, Ramesh T, Pandey KS, et al. Effect of particle size on new constitutive relationship of aluminium–iron powder metallurgy composite during cold upsetting. *Mater Des* 2008; 29: 1011–1026.
- Freudenthal AM. *The inelastic behaviour of solids*. Wiley: New York; 1950.
- Cockcroft MG and Latham DJ. Ductility and workability of metals. *J Inst Metals* 1968; 96: 33–39.
- Oh SI, Chen CC and Kobayashi S. Ductile fracture in axisymmetric extrusion and drawing. Part II. *J Eng Ind* 1979; 101: 36–48.
- Ayada M, Higashino T and Mori K. Central bursting in extrusion of inhomogeneous materials. *Adv Technol Plast* 1987; 1: 553–558.
- Narayana Murty SVS, Nageswara Raob B and Kashyap BP. Improved ductile fracture criterion for cold forming of spheroidised steel. *J Mater Process Technol* 2004; 147: 94–101.
- Banerjee D and Williams JC. Perspectives on titanium science and technology. *Acta Mater* 2013; 61: 844–879.
- Zhang LC and Chen LY. A review on biomedical titanium alloys: recent progress and prospect. *Adv Eng Mater* 2019; 21: 1801215.
- Gupta K and Laubscher RF. Sustainable machining of titanium alloys: a critical review. *Proc IMechE, Part B: J Engineering Manufacture* 2017; 231: 2543–2560.
- Huang C, Zhao Y, Xin S, et al. Effect of microstructure on tensile properties of Ti–5Al–5Mo–5V–3Cr–1Zr alloy. *J Alloys Compd* 2017; 693: 582–591.
- Samal P and Newkirk J. *Powder metallurgy methods and applications*. Materials Park, OH: ASM International, 2015.
- Ahasan MD and Davidson MJ. Modeling aspects of hot densification and deformation studies on Al–TiB₂ composite preforms. *Mater Manuf Processes* 2015; 30: 1190–1195.
- Seetharam R, Kanmani Subbu S and Davidson MJ. Hot workability and densification behavior of sintered powder metallurgy Al–B₄C preforms during upsetting. *J Manuf Process* 2017; 28: 309–218.
- Chakravarthy P, Chakkingal U and Venugopal P. Influence of temperature on the forming limit diagrams of sintered P/M preforms of steel. *Mater Sci Eng A* 2008; 485: 395–402.
- Wolla DW, Davidson MJ and Khanra AK. Studies on the formability of powder metallurgical aluminium–copper composite. *Mater Des* 2014; 59: 151–159.

34. Tharmaraj R and Davidson MJ. Effect of titanium in aluminium matrix on densification and forming limit of P/M composites during upsetting process. *J Braz Soc Mech Sci Eng* 2020; 42.
35. Seetharam R, Kanmani Subbu S and Davidson MJ. Microstructure modeling of dynamically recrystallized grain size of sintered Al-4 wt % B₄C composite during hot upsetting. *J Eng Mater Technol* 2018; 140: 021003-1–021003-8.
36. Seetharam R, Kanmani Subbu S and Davidson MJ. Analysis of grain size evolution of sintered Al-4 wt. % B₄C preforms subjected to hot compression test. *Metallogr Microstruct Anal* 2018; 7: 176–183.

Appendix

Notation

C_1, C_2, C_3, C_4	critical damage parameter
$d\bar{\epsilon}$	effective strain increment
D	initial diameter of the preform
D_b	bulged diameter of the preform
D_{bc}	bottom contact diameter of the deformed preform
D_{tc}	top contact diameter of the deformed preform

F	axial compression load
H	initial height of the preform
H_f	deformed height of the preform
R	relative density
V_{Al-Ti}	volume of P/M Al-Ti preforms
V_v	void volume of deformed P/M Al-Ti preforms
\mathcal{E}_{eff}	effective strain
\mathcal{E}_m	mean (or) hydrostatic strain
\mathcal{E}_z	true axial strain (or) height strain
\mathcal{E}_θ	hoop strain
$\bar{\mathcal{E}}_f$	effective strain at fracture
ν	Poisson's ratio
$\rho_{the,Al-Ti}$	theoretical density of P/M Al-Ti preforms
$\rho_{exp,Al-Ti}$	experimental density of deformed P/M Al-Ti preforms
σ_{eff} or $\bar{\sigma}$	effective stress
σ_m	mean (or) hydrostatic stress
σ_z	true axial stress
σ_θ	hoop stress
σ_1	maximum principal stress